

# Outflows from black hole hyperaccretion systems: short and long-short gamma-ray bursts and “quasi-supernovae”

Cui-Ying Song, Tong Liu<sup>\*</sup>, and Ang Li

*Department of Astronomy, Xiamen University, Xiamen, Fujian 361005, China*

Accepted XXX. Received YYY; in original form ZZZ

## ABSTRACT

The detections of some long gamma-ray bursts (LGRBs) relevant to mergers of neutron star (NS)-NS or black hole (BH)-NS, as well as some short gamma-ray bursts (SGRBs) probably produced by collapsars, muddle the boundary of two categories of gamma-ray bursts (GRBs). In both cases, a plausible candidate of central engine is a BH surrounded by a hyperaccretion disc with strong outflows, launching relativistic jets driven by Blandford-Znajek mechanism. In the framework of compact binary mergers, we test the applicability of the BH hyperaccretion inflow-outflow model on powering observed GRBs. We find that, for a low outflow ratio,  $\sim 50\%$ , postmerger hyperaccretion processes could power not only all SGRBs but also most of LGRBs. Some LGRBs might do originate from merger events in the BH hyperaccretion scenario, at least on the energy requirement. Moreover, kilonovae might be produced by neutron-rich outflows, and their luminosities and timescales significantly depend on the outflow strengths. GRBs and their associated kilonovae are competitive with each other on the disc mass and total energy budgets. The stronger the outflow, the more similar the characteristics of kilonovae to supernovae (SNe). This kind of ‘nova’ might be called ‘quasi-SN’.

**Key words:** accretion, accretion discs - black hole physics - gamma-ray burst: general - magnetic fields - stars: neutron

## 1 INTRODUCTION

Gamma-ray bursts (GRBs) are classified into two categories divided by  $T_{90} \sim 2$  s, i.e., long- and short-duration GRBs (LGRBs and SGRBs, see e.g., Kouveliotou et al. 1993). It is well known that SGRBs are possibly originated from the mergers of neutron star (NS)-NS or black hole (BH)-NS (e.g., Paczyński 1986; Eichler et al. 1989; Paczyński 1991; Popham, Woosley, & Fryer 1999; Narayan, Paczyński, & Piran 1992; Berger 2014), and LGRBs associated with type Ib/c supernovae (SNe) could be powered by collapsars (e.g., Tutukov, Yungelson, & Iben 1992; Galama et al. 1998; Hjorth et al. 2003; Stanek et al. 2003; Woosley & Bloom 2006; Campana et al. 2006; Fruchter et al. 2006; Kumar & Zhang 2015). With the accumulation of observational data, some LGRBs, such as GRB 060614 (e.g., Gehrels et al. 2006; Zhang et al. 2007, 2009), were found to be relevant to mergers, while some SGRBs such as GRB 090426 (e.g., Antonelli et al. 2009; Levesque et al. 2010; Xin et al. 2011) were produced probably by collapsars. Those bursts muddle the LGRB-SGRB boundary. Zhang et al. (2009) summarized the nature of

GRBs and proposed a new classification approach mainly based on their progenitors.

Two types of GRB central engines have been widely discussed: hyper-accreting stellar mass BHs (e.g., Woosley 1993; Lei et al. 2009; Lei, Zhang, & Liang 2013; Liu, Gu, & Zhang 2017a) and rapidly spinning and highly magnetized NSs (magnetars, see e.g., Usov 1992; Thompson 1994; Dai & Lu 1998; Zhang & Mészáros 2001; Dai et al. 2006). The detection of gravitational waves (GWs) from close compact binary mergers (e.g., Eichler et al. 1989; Schutz 1989; Cutler & Flanagan 1994; Lipunov, Postnov, & Prokhorov 1997; Abadie et al. 2010) provides a direct way to verify the progenitors of SGRBs if the association of GWs with SGRBs can be confirmed. After merger events, optical/near-infrared (NIR) emission from the radioactive decay of heavy r-process elements are produced by the merger remains. These transient events are named ‘kilonovae’ (Li & Paczyński 1998). Recently, the NS-NS merger GW event (GW170817) was detected by the advanced LIGO/Virgo collaboration (e.g., Abbott et al. 2017a,b; Alexander et al. 2017; Blanchard et al. 2017; Hallinan et al. 2017; Troja et al. 2017; Shappee et al. 2017). Its electromagnetic counterpart, GRB 170817A accompanied by a kilonova

\* E-mail: tongliu@xmu.edu.cn

AT 2017gfo, was also discovered (e.g., [Abbott et al. 2017c](#); [Chornock et al. 2017](#); [Cowperthwaite et al. 2017](#); [Evans et al. 2017](#); [Kilpatrick et al. 2017](#); [Margutti et al. 2017](#); [Nicholl et al. 2017](#); [Smartt et al. 2017](#)). This event provides the first direct evidence for the progenitor hypothesis of SGRBs.

Outflows may present in accretion processes, especially for super-Eddington accretion discs (e.g., [Shakura & Sunyaev 1973](#)). They were widely studied by theoretical analyses (e.g., [Blandford & Begelman 1999](#); [Liu et al. 2008](#); [Gu 2015](#)), numerical simulations (e.g., [Eggum, Coroniti, & Katz 1988](#); [Okuda 2002](#); [Ohsuga et al. 2005](#); [Ohsuga & Mineshige 2011](#); [Jiang, Stone, & Davis 2014, 2017](#); [McKinney et al. 2014](#); [Sądowski et al. 2014](#); [Sądowski & Narayan 2015](#)), as well as observations (e.g., [Wang et al. 2013](#); [Cheung et al. 2016](#); [Parker et al. 2017a](#)). [Narayan & Yi \(1994\)](#) proposed that the advection-dominated accretion flows (ADAFs) with the positive Bernoulli parameter might generate outflows and, by extension, jets (e.g., [Narayan & Yi 1995](#); [Abramowicz et al. 1995](#)). [Blandford & Begelman \(1999\)](#) emphasized the roles of the outflows in ADAFs and developed a variant named advection-dominated inflow-outflow solution (ADIOS). They also constructed 1D and 2D self-similar solutions and found that the structure and radiation of flows were subject to the outflows ([Blandford & Begelman 2004](#)). As to the study of the vertical structures of the discs, strong outflows were required in both optically-thick and optically-thin flows, resulted from energy equilibrium (e.g., [Gu & Lu 2007](#); [Gu 2015](#)). Outflows can also exist in neutrino-dominated accretion flows (NDAFs, see reviews by [Liu, Gu, & Zhang 2017a](#)). [Liu et al. \(2012a\)](#) visited the vertical structures and luminosities of NDAFs. They found that outflows might be present in the outer region of the discs, depending on the vertical distributions of the Bernoulli parameter.

A wide variety of mechanisms could lead to the generation of outflows. In optically-thick accretion flows, photons could exert radiation pressure upon materials to blow them away. For the optically-thin cases, such as ADAFs, they might possess a positive Bernoulli parameter due to their high internal energy ([Narayan & Yi 1994](#); [Gu 2015](#)). Moreover, the Blandford-Payne process ([Blandford & Payne 1982](#)) could produce outflows for both optically-thin and optically-thick discs (e.g., [Ma et al. 2018](#)).

Apart from theoretical studies, several simulation results also implied that outflows play essential roles in accretion systems. It was first pointed out by [Stone, Pringle, & Begelman \(1999\)](#), where 2D hydrodynamic numerical simulations were carried out. Many later simulations confirmed their conclusion, for example in [Hawley, Balbus, & Stone \(2001\)](#), [Machida, Matsumoto, & Mineshige \(2001\)](#), [Igumenshchev, Narayan, & Abramowicz \(2003\)](#), [Pang et al. \(2011\)](#), and [Yuan & Narayan \(2014\)](#). Furthermore, both the inflow and outflow mass accretion rates decreased inward, following a power-law  $\dot{M} \propto r^s$  ( $0 \leq s \leq 1$ ). For the outflows,  $s \approx 1$  was possible which means that more than 90% of the materials could be pushed into powerful outflows from the accretion disc (e.g., [Yuan, Bu, & Wu 2012](#); [Yuan, Wu, & Bu 2012](#); [Begelman 2012](#)). In the global 3D radiation magneto-hydrodynamical simulation, [Jiang, Stone, & Davis \(2014\)](#) found that the radiation-

driven outflows were formed along the rotation axis and about 20% of the radiative energy were carried by outflows. In a recent study of super-Eddington accretion flows onto supermassive BHs (SMBHs), the outflow speed could approach  $\sim 0.1 - 0.4 c$ , and the mass flux lost could reach 15% – 50% of the net mass accretion rates ([Jiang, Stone, & Davis 2017](#)). The 3D general-relativistic magnetohydrodynamic simulations of NDAFs indicated that the velocities of powerful outflows likely approached  $\sim 0.03 - 0.1 c$  (e.g., [Siegel & Metzger 2017](#)).

Recent observations also showed the importance of outflows in accretion systems. For Galactic SMBH accretion, more than 99% original gas escaped from the disc ([Wang et al. 2013](#)). In quiescent galaxies, [Cheung et al. \(2016\)](#) observed that centrally-driven winds could suppress the star formation. The ultra-fast outflow of the Seyfert I galaxy IRAS 13224-3809 was discovered by [Parker et al. \(2017a\)](#). They also proposed that the outflows could be detected from the long-term X-ray variability ([Parker et al. 2017b](#)). Furthermore, the observed kilonova following GRB 130603B ([Berger, Fong, & Chornock 2013a](#); [Tanvir et al. 2013](#)) might also related to disc winds (e.g., [Metzger & Fernández 2014](#)).

Outflows play important roles in the BH accretion processes, however, few studies have been done on the BH hyperaccretion system. To investigate the nature of the GRB central engine, we necessarily confront the BH hyperaccretion inflow-outflow model with observational data. In paper I, we constrained the characteristics of the progenitor stars of LGRBs and Ultra-LGRBs with the BH hyperaccretion inflow-outflow model in the collapsar scenario ([Liu et al. 2018](#)). In the present work, the applicability of the model is tested to power both SGRBs and LGRBs in the compact binary merger scenario. We further examine the properties of kilonovae triggered by strong neutron-rich outflows. The paper is organized as follows. In Section 2, we describe our BH hyperaccretion inflow-outflow model. The GRB data are presented in Section 3. The properties of kilonovae are shown in Section 4. Section 5 is a brief summary.

## 2 MODEL

There are two types of GRB central engine candidates widely discussed: Magnetar and hyperaccreting BH with stellar mass. After the mergers of NS-NS or BH-NS, an NS with high spin (period  $\sim 1$  ms) and high surface magnetic field ( $\sim 10^{15}$  G) might be formed, known as a millisecond magnetar. The released spin-down energy could power GRBs. Alternatively, in the BH accretion disc models, the GRB jet can be produced either through the neutrino-antineutrino annihilation process (see e.g., [Popham, Woosley, & Fryer 1999](#); [Di Matteo, Perna, & Narayan 2002](#); [Narayan, Piran, & Kumar 2001](#); [Liu et al. 2007](#)), or via the electromagnetic processes.

Some general-relativistic magnetohydrodynamics simulations have showed the evidences for the Blandford-Znajek (BZ) mechanism ([Blandford & Znajek 1977](#); [Blandford & McKee 1977](#)) in GRB central engines (e.g., [Nagataki 2009](#); [Tchekhovskoy & McKinney 2012](#)). [Barkov & Komissarov \(2010\)](#) has confirmed the possibility of the magnetically driven stellar explosions, and

has pointed out the required magnetic flux in excess of  $10^{28}$  G cm<sup>2</sup> in the close compact binary scenario for LGRBs. Moreover, some studies have shown that the BZ mechanism is more efficient than the neutrino annihilation if the magnetic fields are strong enough or the accretion rates are lower than the ignition accretion rates of NDAFs (e.g., Kawanaka, Piran, & Krolik 2013; Liu et al. 2015a; Lei et al. 2017; Liu, Gu, & Zhang 2017a). The BH spin energy might be extracted via the BZ mechanism when a strong magnetic field ( $\sim 10^{13} - 10^{15}$  G) threads the spinning BH and is connected with a distant astrophysical load. Essentially all central engine models require a strong, large-scale magnetic field to launch GRBs. It may inherit and redistribute the large-scale magnetic field of the merging components following the magnetic flux conservation (e.g., Liu et al. 2016; Punsly & Bini 2016).

In the BH hyperaccretion scenario, introducing the effects of the outflows and the relativistic jets driven by the BZ mechanism, the disc model is called BH hyperaccretion inflow-outflow model. Two parameters are required for describing a hyperaccreting stellar mass BH: the dimensionless mass  $m_{\text{BH}} = M_{\text{BH}}/M_{\odot}$  and spin  $a_* \equiv cJ_{\text{BH}}/GM_{\text{BH}}^2$ .

Then the BZ jet power can be estimated as (e.g., Lee, Brown, & Wijers 2000a; Lee, Wijers, & Brown 2000b; Li 2000; McKinney 2005; Barkov & Komissarov 2008; Komissarov & Barkov 2009; Barkov & Komissarov 2010; Lei, Zhang, & Liang 2013)

$$L_{\text{BZ}} = 1.7 \times 10^{50} a_*^2 m_{\text{BH}}^2 B_{\text{BH},15}^2 F(a_*) \text{ erg s}^{-1}, \quad (1)$$

where  $B_{\text{BH},15} = B_{\text{BH}}/10^{15}$  G and  $F(a_*) = [(1+q^2)/q^2][(q+1/q)\arctan(q) - 1]$  with  $q = a_*/(1 + \sqrt{1-a_*^2})$ .

We can evaluate the magnetic field strength when the magnetic pressure on the BH horizon balances the ram pressure of the innermost part of the disc (e.g., Moderski, Sikora, & Lasota 1997)

$$\frac{B_{\text{BH}}^2}{8\pi} = P_{\text{ram}} \sim \rho c^2 \sim \frac{\dot{M}_{\text{in}} c}{4\pi r_{\text{BH}}^2}, \quad (2)$$

where  $r_{\text{BH}} = GM_{\text{BH}}(1 + \sqrt{1-a_*^2})/c^2$  denotes the event horizon of the BH, and  $\dot{M}_{\text{in}}$  is the accretion rate at the inner boundary. Then the magnetic field strength can be written as

$$B_{\text{BH}} \simeq 7.4 \times 10^{16} \dot{m}_{\text{in}}^{1/2} m_{\text{BH}}^{-1} (1 + \sqrt{1-a_*^2})^{-1} \text{ G}. \quad (3)$$

Inserting above equation into Equation (1), we obtain the BZ jet power as a function of mass accretion rate at and spin of BH,

$$L_{\text{BZ}} = 9.3 \times 10^{53} a_*^2 \dot{m}_{\text{in}} X(a_*) \text{ erg s}^{-1}, \quad (4)$$

and

$$X(a_*) = F(a_*)/(1 + \sqrt{1-a_*^2})^2. \quad (5)$$

The dimensionless BH mass accretion rate at the innermost stable orbit  $\dot{m}_{\text{in}}$  is defined as

$$\dot{m}_{\text{in}} = \frac{(1-f)m_{\text{disc}}}{T_{90,\text{rest}}}, \quad (6)$$

where  $T_{90,\text{rest}} = T_{90}/(1+z)$  is the duration of the prompt emission in the rest frame, and  $z$  stands for the redshift.  $m_{\text{disc}} = M_{\text{disc}}/M_{\odot}$  stands for the dimensionless accretion disc mass, and  $f$  represents the fraction of the outflow mass

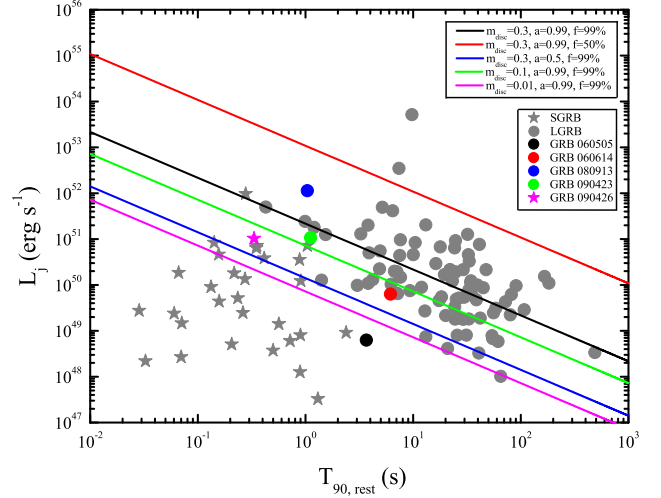


**Figure 1.** Luminosities and timescales of BZ jets originated from compact binary mergers in five solid lines, different colors corresponding to different parameters as labelled. The gray filled stars and circles denote SGRBs and LGRBs data, respectively. The magenta star stands for SGRB that may be related to the collapse of massive stars. The colorful circles are for LGRBs possibly from NS-NS or BH-NS mergers.

to the disc mass. As mentioned in the Introduction, outflows have been found to be very strong in many studies, therefore we take  $f = 99\%$  for the strongest outflow case, and  $f = 50\%$  as a typical value for comparison.

Recently, the simulations of NS-NS mergers (e.g., Dietrich et al. 2015) and BH-NS mergers (e.g., Foucart et al. 2014; Just et al. 2015; Kyutoku et al. 2015; Kiuchi et al. 2015; Siegel & Metzger 2017) showed that the remnant disc mass  $m_{\text{disc}}$  likely possessed an upper limit  $\sim 0.3 M_{\odot}$ , which depends on the equation of state of the NS, the mass ratio, the total mass and the period of the binary (e.g., Oechslin & Janka 2006; Dietrich et al. 2015). We therefore take  $m_{\text{disc}} = 0.01, 0.1, 0.3$  in our calculations.

On the other hand, the jet power can be obtained from the observational data of GRBs (e.g., Fan & Wei 2011; Liu et al. 2015b; Song et al. 2016), i.e.,

$$L_j \simeq \frac{(E_{\gamma,\text{iso}} + E_{\text{k,iso}})(1+z)\theta_j^2}{T_{90}}, \quad (7)$$

where  $E_{\gamma,\text{iso}}$ ,  $E_{\text{k,iso}}$ , and  $\theta_j$  denote the isotropic radiated energy, the isotropic kinetic energy of afterglows, and the jet opening angle, respectively.

### 3 GRB DATA

As shown in Table 1, we collected the data of  $T_{90}$ ,  $z$ ,  $E_{\gamma,\text{iso}}$ ,  $E_{\text{k,iso}}$ ,  $\theta_j$  and the peak energy in the rest frame  $E_{\text{p,rest}}$  of 30 SGRBs and 89 LGRBs. It is worth noting that the measurements of  $E_{\gamma,\text{iso}}$ ,  $E_{\text{k,iso}}$ , and  $\theta_j$  are model dependent. Considerable debates surround the origins of some GRBs due to their perplexing observational phenomena (e.g., Zhang et al. 2009; Xin et al. 2011; Kann et al. 2011; Li, Zhang, & Lü 2016), some unusual GRBs are labelled by the superscript \* in the table, which are shown as following:

**GRB 060505** This burst has a duration of  $4 \pm 1$  s, the

low energy  $\sim 10^{49}$  erg and a very low redshift  $z = 0.0894$ . The presence of a SN is ruled out down to limit of hundreds times fainter than SN 1998bw (Ofek et al. 2007; Fynbo et al. 2006). The star formation rate, metallicity, ionization state of the host environment are more similar to SGRBs than to LGRBs (Levesque & Kewley 2007).

**GRB 060614** Its  $T_{90} \sim 100$  s in the BAT (15–150 keV) band groups it with LGRBs, while its peak luminosity and temporal lag completely satisfy the SGRB subclass (Gehrels et al. 2006). The low-star-formation-rate host galaxy (Savaglio, Glazebrook, & Le Borgne 2009), and its irrelevant to any known SN (Gal-Yam et al. 2006; Fynbo et al. 2006; Della Valle et al. 2006) suggest that it is related to a compact binary merger rather than a collapsar (e.g., Zhang et al. 2007). Furthermore, the discovery of a NIR bump in afterglow denotes the strong connection between GRB 060614 and a kilonova, and provides tangible evidence to support the merger origin (Yang et al. 2015; Jin et al. 2015; Horesh et al. 2016).

**GRB 080913** The burst duration  $T_{90}$  in the BAT band is  $8 \pm 1$  s. Considering its high redshift  $z = 6.7$ , the rest-frame duration of this burst is  $T_{90,\text{rest}} \sim 1$  s. Pal'Shin et al. (2008) fitted the Konus-Wind and the *Swift*/BAT joint spectral analysis, and derived that the best fit peak energies are  $E_{\text{peak}} = 131^{+225}_{-48}$  keV and  $E_{\text{peak}} = 121^{+232}_{-39}$  keV for the cutoff power law and Band-function spectra, respectively. Placing this GRB at  $z = 1$ , it can be classified as SGRBs due to intrinsically short duration and hard spectrum. Pérez-Ramírez et al. (2010) presented the X-ray, NIR and millimetre observations, and proposed that the progenitor of this burst was likely from a BH-NS merger. A maximally-rotating BH might form in the center and power this GRB by the BZ mechanism. However, this GRB is consistent with the lag-luminosity correlation and the Amati relation of LGRBs, which makes the collapsar origin cannot be ruled out (Greiner et al. 2009; Zhang et al. 2009).

**GRB 090423** Similar to GRB 080913, this burst was measured with a high redshift  $z = 8.6$  and a BAT band duration  $T_{90} = 10.3 \pm 1.1$  s. In rest frame, the peak energy and duration are  $491 \pm 200$  keV (Amati, Frontera, & Guidorzi 2009) and  $\sim 1.1$  s, respectively.

**GRB 090426** It is a SGRB with an observed duration of  $T_{90} \sim 1.28$  s at  $z = 2.609$  (Antonelli et al. 2009). On the other hand, the soft spectrum  $E_{p,\text{rest}} = 177^{+90}_{-65}$  keV (Amati, Frontera, & Guidorzi 2009) and burst environment are similar to those of LGRBs. The number density of the medium ( $> 11.2 \text{ cm}^{-3}$ ) is not consistent with the condition of the compact-binary-merger progenitors, which often occur in low density medium (e.g., Xin et al. 2011).

Above all, the observed LGRBs and SGRBs are contaminated by each other. Some studies also found that the duration distributions of SGRBs and LGRBs overlapped each other (e.g., Horváth 2002). Certainly  $T_{90}$  is not a good criterion to manifest the nature of GRBs, which resulted in the old dichotomy between the LGRBs related to collapsars and the SGRBs originated from compact binary mergers.

Figure 1 shows the luminosities and timescales of the BZ jets originated from the compact binary mergers. The solid lines in different colors correspond the BZ jets with the different values of  $m_{\text{disc}}$ ,  $a_*$ , and  $f$ . The gray filled stars and circles denote SGRBs and LGRBs data, respectively. The magenta star stands for the SGRB which may related to the

collapse of massive stars. The colorful circles are for LGRBs possibly from NS-NS or BH-NS mergers. By comparing the red and black lines, one can find that the luminosities of SGRBs decrease when the outflow increases. For  $f = 50\%$ , most of LGRBs find their place under our predicted lines of the BZ jets. For  $f = 99\%$ , at least half of those LGRBs cannot be explained by the model. Therefore, our model can explain not only all SGRBs but also most of LGRBs (with a low outflow ratio).

Actually, assuming that  $T_{90}$  is near or proportional to the duration of the central engine activity, then the duration of GRBs may be closely related to the properties of progenitors. The collapsar scenario is suggested to produce LGRBs through accretion because of the typical envelope fallback timescale is 10 s (e.g., MacFadyen & Woosley 1999). The BH accretion disc systems after NS-NS/BH-NS mergers have a typical accretion timescale  $\sim 0.01 - 0.1$  s, which were raised to account for SGRBs in many models (e.g., Narayan, Piran, & Kumar 2001; Aloy, Janka, & Müller 2005). However, the discover of X-ray flares (e.g., Burrows et al. 2005; Nousek et al. 2006; Wu et al. 2007; Chincarini et al. 2010; Margutti et al. 2010; Mu et al. 2016a,b), extended emission (e.g., Lazzati, Ramirez-Ruiz, & Ghisellini 2001; Connaughton 2002; Norris, Gehrels, & Scargle 2010, 2011; Liu et al. 2012b) and plateaus (e.g., Troja et al. 2007; Rosswog 2007; Rowlinson et al. 2013) in some GRBs denote that the duration of the GRB central engine activity is much longer than  $T_{90}$  in both LGRBs and SGRBs. The gamma-ray duration  $T_{90}$  may much shorter than the central engine activity duration, named ‘tip-of-iceberg’ effect (Lü et al. 2014; Zhang et al. 2014; Li, Zhang, & Lü 2016; Gao et al. 2017a; Liu et al. 2018). A longer accretion timescale is needed to explain these observations by the BH hyperaccretion systems. The durations of the compact binary mergers are not necessarily to be ‘short’, and in principle the collapsar model can also bring forth SGRBs (e.g., Janiuk & Proga 2008; Zhang et al. 2009). If it is the case, the values of the jet luminosities and timescales of GRBs are larger than these in Table 1. Thus the admission of the model limitations is stricter than in the current situations.

#### 4 QUASI-SNE

As strong GW sources in the nearby galaxies, the NS-NS/BH-NS mergers are expected to have electromagnetic counterparts such as SGRBs (e.g., Eichler et al. 1989; Nakar 2007; Berger 2014; Kumar & Zhang 2015; Levan et al. 2016), off-axis emission of SGRB jets (e.g., Rhoads 1999; Lazzati et al. 2017; Xiao et al. 2017), optical/NIR signals powered by the decay of heavy radioactive elements in the ejection matter (e.g., Li & Paczyński 1998; Metzger 2017), radio flares (e.g., Nakar & Piran 2011; Gao et al. 2013; Piran, Nakar, & Rosswog 2013), or X-ray emission from GRB central engine (e.g., Nakamura et al. 2014; Kisaka, Ioka, & Nakamura 2015). Furthermore, Zhang (2013) proposed that potentially an early X-ray afterglow would continue for thousands of seconds followed GW bursts once the NS-NS merger produced a magnetar rather than a BH. So the existence of an X-ray transient might be used as a criterion to judge if it is a remnant magnetar. The BH sce-

**Table 1.** GRBs data

Name	$T_{90}$	$z$	$E_{\gamma, \text{iso}}$	$E_{\text{k, iso}}$	$E_{\text{p, rest}}$	$\theta_j$	$L_j$	Ref
	(s)	$z$	( $10^{52}$ erg)	( $10^{52}$ erg)	(keV)	(rad)	( $10^{50}$ erg s $^{-1}$ )	
SGRBs								
050509B	0.04	0.225	$0.00024^{+0.00044}_{-0.0001}$	0.0055	$100.45^{+748.475}_{-98}$	$> 0.05$	0.022	1, 2
050709	0.07	0.161	$0.0027 \pm 0.0011$	0.0016	$96.363^{+20.898}_{-13.932}$	$> 0.26$	0.2397	1, 3
050724A	3	0.257	$0.009^{+0.011}_{-0.002}$	0.027	$138.27^{+502.8}_{-56.565}$	$> 0.35$	0.0915	1, 2
051210	1.3	1.3	$0.4^{+0.5}_{-0.2}$	0.238	$943^{+1495}_{-598}$	$> 0.05$	0.1411	1, 2
051221A	1.4	0.5465	$0.28^{+0.21}_{-0.1}$	1.26	$603.135^{+1020.69}_{-293.835}$	0.12	1.2234	1, 2
060502B	0.09	0.287	$0.003^{+0.005}_{-0.002}$	0.012	$437.58^{+926.64}_{-244.53}$	$> 0.05$	0.0268	1, 2
060801	0.5	1.13	$0.7^{+1.5}_{-0.5}$	0.071	$1320.6^{+2279.1}_{-724.2}$	$0.0561^{+0.0056}_{-0.0063}$	0.5167	1, 2, 4
061006	0.4	0.438	$3^{+4}_{-1}$	0.314	$819.66^{+1308.58}_{-402.64}$	$0.407^{+0.068}_{-0.173}$	97.3211	1, 2, 4
061201	0.8	0.111	$3^{+4}_{-2}$	0.007	$666.6^{+888.8}_{-388.85}$	0.017	0.0603	1, 2
061210	0.2	0.409	$0.09^{+0.16}_{-0.05}$	0.086	$760.86^{+1070.84}_{-436.79}$	$> 0.37$	8.3909	1, 2, 5
070429B	0.5	0.902	$0.07^{+0.11}_{-0.02}$	0.451	$228.24^{+1418.89}_{-125.532}$	$> 0.05$	0.2477	1, 2
070714B	2.0	0.923	$1.16^{+0.41}_{-0.22}$	0.232	$2153.76^{+1499.94}_{-730.74}$	$0.33^{+0.11}_{-0.11}$	7.2217	1, 3, 4
070724A	0.4	0.457	$0.003 \pm 0.001$	0.099	99	$0.27^{+0.16}_{-0.16}$	1.346	1, 3, 4
070729	0.9	0.8	0.017	0.132	$840.6^{+1526}_{-351}$	$> 0.05$	0.0372	1, 6
070809	1.3	0.473	0.0056	0.391	$75.6^{+12.6}_{-13.9}$	$0.4^{+0.08}_{-0.333}$	3.5473	1, 4, 6
071227	1.8	0.381	$0.1 \pm 0.02$	0.025	$1384 \pm 277$	$> 0.0262$	0.0033	1, 5, 7
080905A	1.0	0.122	0.0005	0.0024	$502.8^{+950.6}_{-280.5}$	$0.28^{+0.15}_{-0.16}$	0.0127	1, 4, 6
090426*	1.2	2.609	$0.5 \pm 0.1$	13.5	$177^{+90}_{-65}$	0.07	10.3115	1, 8
090510	0.3	0.903	$4.47^{+4.06}_{-3.77}$	0.307	$7490^{+532.8}_{-497.4}$	0.017	0.4379	1, 6
090515	0.04	0.403	0.0008	0.062	$90.1^{+47.4}_{-16.8}$	$> 0.05$	0.2753	1, 6
100117A	0.3	0.92	$0.09 \pm 0.01$	0.11	$551^{+142}_{-96}$	$0.27^{+0.15}_{-0.15}$	4.6373	1, 4, 7
100206A	0.1	0.408	$0.0763^{+0.0789}_{-0.0229}$	0.0073	$638.98^{+131.21}_{-131.21}$	$> 0.05$	0.1471	1, 9
100625A	0.3	0.453	$0.075 \pm 0.003$	0.0093	$701.32 \pm 114.71$	$> 0.05$	0.051	1, 10
101219A	0.6	0.718	$0.49 \pm 0.07$	0.045	$842^{+177}_{-136}$	$0.29^{+0.14}_{-0.14}$	6.3966	1, 4, 7
111117A	0.5	1.3	$0.338 \pm 0.106$	0.377	$966 \pm 322$	0.105	1.8114	1, 10
120804A	0.81	1.3	0.7	0.7	$310.5^{+151.8}_{-66.7}$	$> 0.19$	7.1539	11
130603B	0.18	0.356	$0.212 \pm 0.023$	0.28	$900 \pm 140$	0.07	0.9077	1, 10
131001A	1.54	0.717	0.037	0.541	$94.44 \pm 24.04$	$> 0.05$	0.0805	1, 12
140622A	0.13	0.959	0.0065	0.977	$86.2 \pm 15.67$	$> 0.05$	1.8522	1, 13
160821B	0.48	0.16	$0.021 \pm 0.002$	8	$97.44 \pm 22.04$	0.063	3.8455	14, 15

nario will not fit the data in this case (Sun, Zhang, & Gao 2017).

As mentioned above, the compact objects merger model is accompanied by the ejection of neutron-rich matter. The dynamical ejecta, in a typical timescale of milliseconds, constitute contact-interface materials which are squeezed out by the hydrodynamic force (e.g., Oechslin, Janka, & Marek 2007; Bauswein, Goriely, & Janka 2013; Hotokezaka et al. 2013) or the tidal force (e.g., Kawaguchi et al. 2015). For NS-NS mergers, the typical ejecta velocity and mass are in the range of  $\sim 0.1 - 0.3 c$  and  $\sim 10^{-4} - 10^{-2} M_{\odot}$ , respectively (e.g., Hotokezaka et al. 2013). Recent BH-NS merger simulations revealed that the ejecta mass could reach  $0.1 M_{\odot}$  with a similar velocity as in the NS-NS cases (Kawaguchi et al. 2015, 2016). Then heavy radioactive elements will form via the r-process of neutron-rich matter. The radioactive decay of these elements provides a source for powering transient optical/NIR emission (Eichler et al. 1989; Li & Paczyński 1998), named ‘kilonova’ (Kulkarni 2005) [also called ‘macronova’ (Metzger et al. 2010)].

In addition to the radioactivity of the merger ejecta, the remnant materials’ fall-back accretion (e.g., Rosswog 2007; Rossi & Begelman 2009; Chawla et al. 2010; Kyutoku et al. 2015), the ejecta from the disc, like winds

(e.g., Metzger & Berger 2012; Ma et al. 2018) or outflows, and magnetars (e.g., Zhang 2013; Gao et al. 2013; Yu, Zhang, & Gao 2013; Metzger & Piro 2014; Gao et al. 2015, 2017b; Yi et al. 2017, 2018) can also power kilonovae. For some SGRBs with extended emission or internal X-ray plateaus, the magnetars might form after NS-NS mergers and provide the additional energy injection into the ejecta to power ‘mergernovae’ (e.g., Yu, Zhang, & Gao 2013). In this paper, the nature of the outflows represents the heavy-nuclei-dominated injections into kilonovae.

The kilonovae are claimed to be detected in the optical/NIR band, associated with some GRBs, i.e., GRBs 050709 (Jin et al. 2016), 060614 (Yang et al. 2015; Jin et al. 2015; Horesh et al. 2016), 130603B (Tanvir et al. 2013; Berger, Fong, & Chornoc 2013a; Fan et al. 2013), and 160821B (Kasliwal et al. 2017). The excess optical emission was also discovered in GRB 080503 with a lack of redshift (Perley et al. 2009). Gao et al. (2017b) revisited the *Swift* SGRB samples and found three ‘magnetar-powered merger-nova’ candidates, i.e., GRBs 050724, 070714B, and 061006. The luminosities of these sources are ten times or a hundred times higher than those of typical kilonovae. For the recent GW event, the luminosity of GRB 170817A is one order of

Table 1 – *continued*

Name	$T_{90}$	$z$	$E_{\gamma, \text{iso}}$	$E_{k, \text{iso}}$	$E_{p, \text{rest}}$	$\theta_j$	$L_j$	Ref
	(s)	$z$	( $10^{52}$ erg)	( $10^{52}$ erg)	(keV)	(rad)	( $10^{50}$ erg s $^{-1}$ )	
LGRBs								
970508	14.0 ± 3.6	0.8349	0.61 ± 0.13	0.99 ± 0.14	145 ± 43	0.3775 ± 0.0291	1.4765	16, 17
970828	160.0	0.96	29 ± 3	37.154	586 ± 117	0.1239	0.6212	16, 18
971214	31.23 ± 1.18	3.418	21 ± 3	8.48 ± 0.97	685 ± 133	> 0.0967 ± 0.0040	1.9483	16, 17
980613	42.0 ± 22.1	1.0964	0.59 ± 0.09	1.22 ± 0.38	194 ± 89	> 0.2194 ± 0.0101	0.2166	16, 17
980703	76.0 ± 10.2	0.966	7.2 ± 0.7	2.41 ± 0.63	503 ± 64	0.1957 ± 0.0141	0.4745	16, 17
990123	63.3 ± 0.3	1.61	229 ± 37	534	1724 ± 446	0.064 ± 0.005	6.4408	16, 19
990510	67.58 ± 1.86	1.619	17 ± 3	13.16 ± 1.12	423 ± 42	0.0586 ± 0.0037	0.2006	16, 17
990705	32.0 ± 1.4	0.84	18 ± 3	0.34 ± 0.12	459 ± 139	0.0930 ± 0.0072	0.4557	16, 17
991216	15.17 ± 0.091	1.02	67 ± 7	36.64 ± 1.79	648 ± 134	0.0798 ± 0.0126	4.3918	16, 17
000210	9.0 ± 1.4	0.846	14.9 ± 1.6	0.50 ± 0.12	753 ± 26	> 0.1194 ± 0.0049	2.2489	16, 17
000926	1.30 ± 0.59	2.0387	27.1 ± 5.9	9.97 ± 3.75	310 ± 20	0.1075 ± 0.0054	50.0191	16, 17
010222	74.0 ± 4.1	1.4769	81 ± 9	22.79 ± 2.48	766 ± 30	0.0559 ± 0.0023	0.5426	16, 17
011211	51.0 ± 7.6	2.14	5.4 ± 0.6	71.32 ± 0.22	186 ± 24	0.1114 ± 0.0070	2.9279	16, 17
020813	89	1.25	66 ± 16	204.174	590 ± 151	0.0541	0.9993	16, 18
021004	77.1 ± 2.6	2.3304	3.3 ± 0.4	8.35 ± 1.45	266 ± 117	0.2211 ± 0.0787	1.225	16, 17
050126	30	1.29	0.8 $^{+1.0}_{-0.2}$	39.8 ± 80.4	387.01 $^{+1135.84}_{-144.27}$	0.365 $^{+0.095}_{-0.125}$	20.4159	2, 4, 20
050315	96 ± 10	1.9500	5.7 $^{+6.2}_{-0.1}$	512.403 $^{+45.299}_{-65.577}$	126.85 $^{+32.45}_{-123.9}$	0.0759 $^{+0.0080}_{-0.0091}$	4.5837	2, 17
050318	32 ± 2	1.4436	2.2 ± 0.16	11.259 $^{+0.867}_{-0.685}$	115 ± 25	0.0380 ± 0.0070	0.0742	16, 17
050319	139.4 ± 8.2	3.2425	4.6 $^{+6.5}_{-0.6}$	77.896 $^{+20.496}_{-28.695}$	190.912 $^{+114.548}_{-182.428}$	0.0380 $^{+0.0051}_{-0.0070}$	0.1812	2, 17
050401	38	2.9	35 ± 7	4570.9 ± 1317.6	467 ± 110	0.472 $^{+0.02}_{-0.044}$	5168.5851	4, 16, 20
050416A	5.4	0.654	0.1 ± 0.01	15.1 ± 3.9	25.1 ± 4.2	0.237 $^{+0.114}_{-0.059}$	13.0142	4, 16, 20
050505	63 ± 2	4.27	16 $^{+13}_{-3}$	237.829 $^{+98.405}_{-49.203}$	737.8 $^{+1807.61}_{-226.61}$	0.0290 $^{+0.0059}_{-0.0030}$	0.8928	2, 17
050525	11.5	0.606	2.5 ± 0.43	28.2 ± 8.1	127 ± 10	0.0551 $^{+0.0069}_{-0.0062}$	0.6507	4, 16, 20
050730	155 ± 20	3.97	9 $^{+8}_{-3}$	86.1223	974.12 $^{+2798.11}_{-432.39}$	> 0.023	0.0807	2, 19
050802	20	1.71	1.8197 $^{+1.6477}_{-0.30614}$	616.6 ± 295.4	268.3 $^{+623.3}_{-75.9}$	0.29 $^{+0.15}_{-0.15}$	349.8991	4, 20, 21
050814	48	5.3	6 $^{+3}_{-1}$	831.764	403.2 $^{+378}_{-138.6}$	0.0419	9.6506	2, 18
050820A	600	2.615	97.4 ± 7.8	53.7145	1325 ± 277	0.184	1.5369	16, 19
050904	183.6 ± 13.2	6.295	124 ± 13	88.37 $^{+86.3}_{-44.2}$	3178 ± 1094	0.0340 ± 0.0051	0.4877	16, 17
050922C	4.5	2.198	5.3 ± 1.7	47.725	415 ± 111	0.026	1.2736	16, 19
051109A	360	2.35	6.5 ± 0.7	169.824	539 ± 200	0.0593	0.2884	16, 18
060124	298 ± 2	2.297	41 ± 6	578.87 $^{+110.79}_{-12.66}$	784 ± 285	0.0531 $^{+0.0091}_{-0.0040}$	0.9666	16, 17
060206	5.0 ± 0.7	4.05	4.3 ± 0.9	386.76 ± 93.02	394 ± 46	0.0351 ± 0.0010	24.3279	16, 17
060210	220 ± 70	3.91	42 $^{+35}_{-8}$	1313.2261	667.76 $^{+1703.77}_{-191.49}$	0.024 ± 0.002	0.871	2, 19
060418	52 ± 1	1.49	13 ± 3	7.5307	572 ± 143	0.029 ± 0.006	0.0413	16, 19
060505*	4 ± 1	0.089	0.0012 ± 0.0002	0.028	482.4 $^{+524.8}_{-167.7}$	~ 0.4	0.06275	6, 22, 23
060526	258.8 ± 5.4	3.21	2.6 ± 0.3	15.58 $^{+0.24}_{-0.21}$	105 ± 21	0.0630 ± 0.0010	0.0587	16, 17
060605	19 ± 1	3.8	2.5 $^{+3.1}_{-0.6}$	115	681.6 $^{+1723.2}_{-240}$	> 0.046	3.14	2, 19
060607A	100 ± 5	3.082	9 $^{+7}_{-2}$	0.822	567.398 $^{+889.876}_{-167.362}$	> 0.095	0.1808	2, 19
060614*	6.9	0.12	0.21 ± 0.09	1.698	55 ± 45	0.2025	0.6328	16, 18
060707	210.0	3.42	5.4 ± 1	102.329	279 ± 28	0.1379	2.1525	16, 18
060714	108.2 ± 6.4	2.71	7.7 $^{+7.5}_{-0.9}$	250.46 ± 248.11	196.63 $^{+348.74}_{-181.79}$	0.0201 ± 0.0010	0.1788	2, 17
060908	18.0 ± 0.8	1.8836	9.8 ± 0.9	2017.68 $^{+2522.09}_{-504.42}$	514 ± 102	0.0080 $^{+0.0051}_{-0.0010}$	1.0394	16, 17
061007	75 ± 5	1.262	86 ± 9	29.9425	890 ± 124	> 0.138	3.3244	16, 19
061021	79.0	0.35	10 $^{+8}_{-4}$	6.166	661.5 $^{+985.5}_{-337.5}$	0.1501	0.3106	2, 18
061121	81 ± 5	1.314	22.5 ± 2.6	20.5215	1289 ± 153	0.099	0.6018	16, 19
061222A	16.0	2.09	21 $^{+11}_{-4}$	2290.868	710.7 $^{+747.78}_{-210.12}$	0.0471	49.5146	2, 18
070110	89 ± 7	2.352	3.0 $^{+2.5}_{-0.5}$	0.687	372.072 $^{+1035.77}_{-90.504}$	> 0.274	0.518	2, 19
070125	63.0 ± 1.7	1.5477	80.2 ± 8	6.43 $^{0.9}_{0.17}$	934 ± 148	0.2304 ± 0.0105	9.2574	16, 17
070306	3.0	1.5	6 $^{+5}_{-1}$	67.608	300 $^{+1340}_{-97.5}$	0.0768	18.081	2, 18
070318	63 ± 3	0.84	0.9 $^{+0.9}_{-0.2}$	47.2719	360.64 $^{+818.8}_{-143.52}$	0.127 ± 0.008	1.1331	2, 19
070411	101 ± 5	2.95	10 $^{+8}_{-2}$	83.6596	474 $^{+2196.2}_{-154.05}$	0.032 ± 0.005	0.1875	2, 19
070508	23.4	0.82	8 $^{+2}_{-1}$	10.715	378.56 $^{+138.32}_{-74.62}$	0.0611	0.2716	2, 18
071010A	6 ± 1	0.98	0.13 ± 0.01	7.2164	73 $^{+97.7}_{-69.9}$	0.090 ± 0.008	0.9812	19, 21
071010B	35.7 ± 0.5	0.947	1.7 ± 0.9	7.2713	101 ± 20	0.150 ± 0.006	0.5494	16, 19
071031	150.5	2.692	3.9 ± 0.6	1.554	45.23 $^{+22.85}_{-41.54}$	0.070 ± 0.013	0.0328	19, 21

Table 1 – continued

Name	$T_{90}$	$z$	$E_{\gamma,iso}$	$E_{k,iso}$	$E_{p,rest}$	$\theta_j$	$L_j$	Ref
	(s)	$z$	( $10^{52}$ erg)	( $10^{52}$ erg)	(keV)	(rad)	( $10^{50}$ erg s $^{-1}$ )	
080310	32.0	2.43	6.0256	29.512	$75.4^{+72}_{-30.8}$	0.0628	0.7509	18, 21
080319C	29.55	1.95	$14.1 \pm 2.8$	74.4078	$906 \pm 272$	$> 0.102$	4.5924	16, 19
080330	$61 \pm 9$	1.51	$0.21 \pm 0.05$	21.0923	$< 88$	$> 0.087$	0.3315	19, 24
080413B	8.0	1.1	$2.4 \pm 0.3$	138.038	$150 \pm 30$	0.1047	20.1874	18, 25
080603A	150	1.688	$2.2 \pm 0.8$	52.5129	$160^{+920}_{-130}$	$0.071 \pm 0.011$	0.247	19, 26
080710	$120 \pm 17$	0.845	$0.8 \pm 0.4$	2.6451	200	$> 0.062$	0.0102	19, 27
080810	$108 \pm 5$	3.35	$45 \pm 5$	41.8519	$1470 \pm 180$	$> 0.105$	1.9266	19, 25
080913*	$8 \pm 1$	6.695	$8.6 \pm 2.5$	$\leq 10$	$710 \pm 350$	$0.359^{+0.125}_{-0.099}$	114.0568	4, 25
081008	$162.2 \pm 25.0$	1.967	$9.98^{+2.34}_{-2.31}$	$134.7^{+18.3}_{-17.3}$	$255.9 \pm 57.47$	$0.0227 \pm 0.0070$	0.0682	17, 28
081203A	223	2.1	$35 \pm 3$	11.2261	$1541 \pm 757$	$> 0.116$	0.4319	19, 29
081222	5.8	2.77	$30 \pm 3$	131.826	$505 \pm 34$	0.0489	12.5737	18, 25
090313	$78 \pm 19$	3.375	3.2	276.8523	$240.1^{+885.4}_{-223.5}$	$> 0.093$	6.7881	19, 21
090323	$133.1 \pm 1.4$	3.568	$410 \pm 50$	$116^{+13}_{-9}$	$1901 \pm 343$	$0.0489^{+0.0070}_{-0.0017}$	2.1579	17, 25
090328	$57 \pm 3$	0.7354	$13 \pm 3$	$82^{+28}_{-18}$	$1028 \pm 312$	$0.0733^{+0.0227}_{-0.0140}$	0.7767	17, 25
090423*	$10.3 \pm 1.1$	8.23	$11 \pm 3$	$340^{+110}_{-140}$	$491 \pm 200$	$0.0262^{+0.0122}_{-0.0052}$	10.7949	17, 25
090424	$49.47 \pm 0.9$	0.544	$4.6 \pm 0.9$	53.1215	$273 \pm 50$	$> 0.378$	12.718	19, 25
090812	75.9	2.452	$40.3 \pm 4$	148.827	$2023 \pm 663$	$> 0.071$	2.1671	19, 29
090902B	$19.328 \pm 0.286$	1.8829	$1.77 \pm 0.01$	$56^{+3}_{-7}$	$596.76 \pm 17.2974$	$0.0681 \pm 0.0035$	1.9973	3, 17
090926A	$20 \pm 2$	2.1062	$210^{+9}_{-8}$	$6.8 \pm 0.2$	$1279.75 \pm 62.124$	$0.1571^{+0.0698}_{-0.0349}$	41.4656	3, 17
091018	106.5	0.97	0.5888	12.023	$51.29 \pm 23.7$	0.0820	0.0784	18, 28
091020	65	1.71	$12.2 \pm 2.4$	51.286	$129.809 \pm 19.241$	0.1204	1.9162	7, 18
091024	1020	1.092	$28 \pm 3$	37.2529	$794 \pm 231$	$> 0.071$	0.0337	19, 29
091029	39.2	2.752	$7.4 \pm 0.74$	40.303	$230 \pm 66$	$> 0.192$	8.39	19, 29
091208B	71	1.063	$2.01 \pm 0.07$	50.119	$297.4846^{+37.13}_{-28.6757}$	0.1274	1.2276	7, 18
100418A	$8.0 \pm 2.0$	0.6235	$0.99^{+0.63}_{-0.34}$	3.36	$47.08^{+3.247}_{-43.83}$	0.3560	5.5352	30, 31
100621A	$63.6 \pm 1.7$	0.542	$4.37 \pm 0.5$	111.7596	$146 \pm 23.1$	$> 0.234$	7.6734	19, 29
100728B	$12.1 \pm 2.4$	2.106	$2.66 \pm 0.11$	95.665	$406.886 \pm 46.59$	$> 0.063$	5.0071	7, 19
100901A	439	1.408	6.3	167.3233	230	0.152	1.098	19, 32
100906A	$114.4 \pm 1.6$	1.727	$28.9 \pm 0.3$	23.8173	$289.062^{+47.72}_{-55.0854}$	$0.055 \pm 0.002$	0.19	7, 19
110205A	$257 \pm 25$	2.22	$56 \pm 6$	31.2172	$715 \pm 239$	0.064	0.2237	19, 29
110213A	$48 \pm 6$	1.46	$6.9 \pm 0.2$	25.7527	$242.064^{+20.91}_{-16.974}$	$> 0.142$	1.6843	7, 19
120119A	$70 \pm 4$	1.728	36	4.17	$498.9 \pm 22.31$	$0.032 \pm 0.002$	0.0801	19, 28
120326A	$11.8 \pm 1.8$	1.798	$3.2 \pm 0.1$	$14.0 \pm 0.07$	$152 \pm 14$	$0.0803 \pm 0.0035$	1.3142	17, 33
120521C	$26.7 \pm 0.4$	6	$8.25^{+2.24}_{-1.96}$	$22^{+37}_{-14}$	$682^{+845}_{-207}$	$0.0524^{+0.0401}_{-0.0192}$	1.0885	17, 34

Notes:

\* GRBs have unusual characteristics on observations (Xin et al. 2011; Zhang et al. 2009).

References:

(1) Liu et al. 2015a; (2) Butler et al. 2007; (3) Zhang et al. 2011; (4) Ryan et al. 2015; (5) Racusin et al. 2009; (6) Kann et al. 2011; (7) Zhang et al. 2012; (8) Antonelli et al. 2009; (9) Tsutsui et al. 2013; (10) Zaninoni et al. 2016; (11) Berger et al. 2013; (12) Cummings et al. 2013; (13) Sakamoto et al. 2014; (14) Stanbro & Meegan 2016; (15) Lü et al. 2017; (16) Amati et al. 2008; (17) Song et al. 2016; (18) Nemmen et al. 2012; (19) Yi et al. 2016; (20) Zhang et al. 2007; (21) Kann et al. 2010; (22) Xu et al. 2009; (23) Ofek et al. 2007; (24) Guidorzi et al. 2009; (25) Amati, Frontera, & Guidorzi 2009; (26) Guidorzi et al. 2011; (27) Krühler et al. 2009; (28) Dichiara et al. 2016; (29) Ghirlanda et al. 2012; (30) Marshall et al. 2011; (31) Laskar et al. 2015; (32) Gorbvskoy et al. 2012; (33) Demianski et al. 2017; (34) Yasuda et al. 2017.

magnitude lower than that of associated AT 2017gfo (e.g., Smartt et al. 2017).

as

$$\begin{aligned}
 t_c &= \left( \frac{3\kappa f M_{\text{disc}}}{4\pi V^2} \right)^{1/2} \\
 &= 1.13 \text{ day} \left( \frac{f M_{\text{disc}}}{0.01 M_{\odot}} \right)^{1/2} \left( \frac{3V}{c} \right)^{-1} \left( \frac{\kappa}{\kappa_e} \right)^{1/2}, \quad (8)
 \end{aligned}$$

The outflow matter is much massive than the dynamical ejecta after mergers, so we just calculated the effects of the outflows on kilonovae. Following Li & Paczyński (1998), we adopt a power law decay model here, and assume the material envelope expanding uniformly with the fixed velocity  $V$ , constant outflow mass  $M_{\text{outflow}} = f M_{\text{disc}}$ , surface radius  $R$ , and density  $\rho$ . The critical time  $t_c$ , when the optical depth of the expanding sphere satisfies  $\kappa \rho R = 1$ , can be calculated

where  $\kappa \sim \kappa_e$  and  $\kappa_e \sim 0.1 \text{ cm}^2 \text{ g}^{-1}$  (e.g., Metzger et al. 2010) represent the average opacity and the electron scattering, respectively, and  $V = 0.1 c$  is adopted. As shown in Figures 1 and 2, we take  $m_{\text{disc}} = 0.3, 0.1, 0.01$ , and  $f = 99\%, 50\%$  to demonstrate the budget on the outflow strength and remnant inflow mass to kilonovae and GRBs. The luminosity of

a kilonova powered by the radioactive decay of nuclei can be estimated as

$$L_{\text{kilo}} = L_0 \sqrt{\frac{8\beta}{3}} Y \left( \sqrt{\frac{3}{8\beta}} \tau \right), \quad (9)$$

where  $L_0 = 3\eta f M_{\text{disc}} c^2 / (4\beta t_c)$ ,  $\tau = t/t_c$ , and  $\beta = V/c$ .  $\eta = 3 \times 10^{-6}$  denotes the fraction of rest-mass energy released in radioactive decay (Metzger et al. 2010), and  $Y(x) = e^{-x^2} \int_0^x e^{k^2} dk$  is the Dawson's integral.

By assuming blackbody emission, the effective temperature of the thermal emission is given by

$$T_{\text{eff}} = \left( \frac{L_{\text{kilo}}}{4\pi\sigma R_{\text{ph}}^2} \right)^{1/4}, \quad (10)$$

where  $\sigma$  is the Stephan-Boltzmann constant, and  $R_{\text{ph}}$  is the photosphere radius corresponding to the radius of mass shell when the optical depth is equal to 1.

The flux density of the source at photon frequency  $\nu$  can be described as follows,

$$F_\nu = \frac{2\pi h\nu^3}{c^2} \frac{1}{e^{h\nu/kT_{\text{eff}}} - 1} \frac{R_{\text{ph}}^2}{D^2}. \quad (11)$$

Then we can get the luminosity of an observational frequency  $\nu$ , i.e.,

$$\nu L_\nu = \nu 4\pi D^2 F_\nu = \frac{8\pi^2 h\nu^4 R_{\text{ph}}^2}{c^2} \frac{1}{e^{h\nu/kT_{\text{eff}}} - 1}. \quad (12)$$

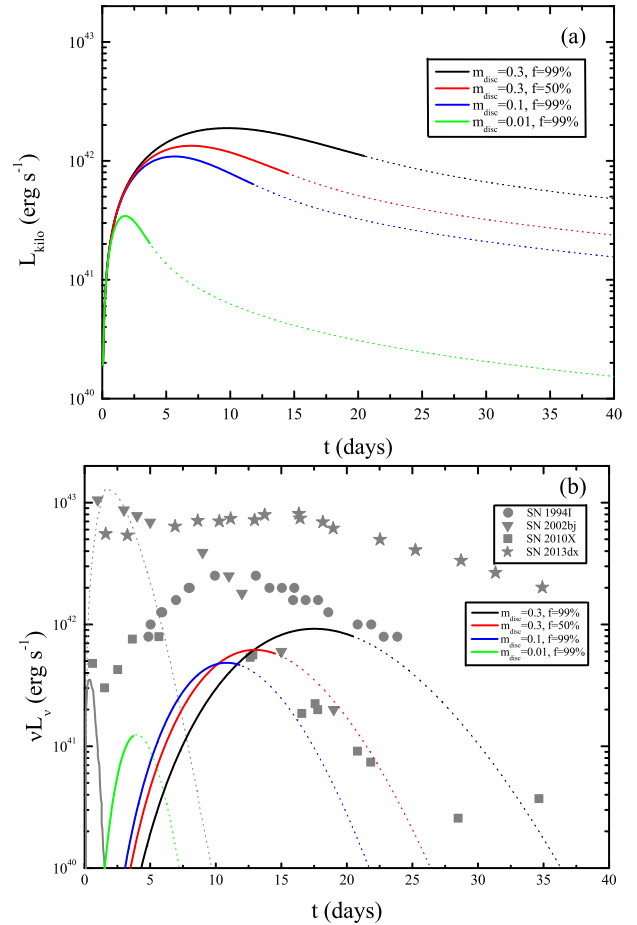
The total luminosities of kilonovae are shown in Figure 2(a). Lines in different color (black, red, blue, green) correspond to different values of  $m_{\text{disc}}$ , and  $f$ . Thick solid parts and thin dotted parts indicate the expanding spheres in the optically-thick and optically-thin, respectively. We notice that the luminosities of kilonovae increase with the increase of the outflow ratios and residual masses.

Figure 2(b) displays the optical ( $\sim 1$  eV) light curves of kilonovae, in comparison with SNe and mergernovae. The gray filled stars and circles respectively represent the data of SN 2013dx and SN 1994I. The grey solid and dashed lines depict the optical light curves of the millisecond-magnetar-powered mergernovae, which are adapted from Figure 3 in Yu, Zhang, & Gao (2013).

From Figure 1 and Figure 2, one can conclude that the energies of a GRB and its associated kilonova appear to be complementary to each other, mainly depending on the neutron-rich outflow ratio. Comparing those light curves, we find that for strong outflows and massive remnants, the durations of the kilonovae powered by the outflows are much longer than those of mergernovae, even approaching those of SNe. That is, the more massive accretion materials become the outflows, the more similar the behaviours of kilonovae become faint SNe, especially the SNe with the steep decay such as SN 2002bj and SN 2010X. Therefore, we prefer the name ‘quasi-SNe’ for these phenomena, and we expect that a new type of ‘nova’ like the faint SNe may be detected after merger events. In addition, the vertical distribution of the outflows might effect the luminosity of the kilonovae for different view angles.

## 5 SUMMARY

The progenitors of GRBs remain mysteries after about fifty years’ discussions. It is still difficult to identify the physical



**Figure 2.** (a) Total luminosity of kilonovae. (b) Comparisons of the optical ( $\sim 1$  eV) light curves with SNe and mergernovae. Lines in different colors (black, red, blue, green) correspond to different values of  $m_{\text{disc}}$  and  $f$ . Thick solid parts and thin dotted parts indicate the expanding spheres in the optically-thick and optically-thin, respectively. The gray filled circles, triangles, squares, and stars represent SN 1994I, SN 2002bj, SN 2010X, and SN 2013dx data, respectively. The grey solid and dashed lines depict optical light curves of the millisecond-magnetar-powered mergernovae Yu, Zhang, & Gao (2013)

origin of a GRB with multi-wavelength observational data available. The traditional definition of SGRBs and LGRBs by  $T_{90}$  might not shed light on their progenitors.

After the mergers of NS-NS or BH-NS, a BH might be born surrounded by a hyperaccretion disc. In the present work, we test the applicability of the BH hyperaccretion inflow-outflow model on powering both LGRBs and SGRBs in the compact binary merger scenario. If about half of the disc materials become outflows, the luminosity and duration of the hyperaccretion processes might satisfy the requirements of not only all SGRBs but also account for most of LGRBs. We also point out that, to verify the origin of GRBs one may need various information, including the characteristics of host galaxies, the SN associations, and the spectral lags, etc.

The optical/NIR emission observed in GRB afterglows are possibly powered by the numerous energy sources (for reviews, see e.g., Metzger 2017). Here we propose a new mechanism of a BH hyperaccretion disc with extreme strong

neutron-rich outflows, named quasi-SNe. The luminosities and timescales of quasi-SNe depend significantly on the outflow strengths. Consequently, there is a severe competition between GRBs and the associated quasi-SNe on the disc mass and energy budgets. In contrast, the luminosity of a mergernova depend on the energy injection from a magnetar, and there is no obvious correlation between it and the GRB luminosity, since most of the spin-down energy would be dissipated via GW emission (e.g., Liu et al. 2017). In the particular case of GRB 170817A and AT 2017gfo, our model can naturally explain a weak GRB associated by a bright kilonova by considering the vertical distribution of the outflows, even without an off-axis jet for observers (e.g., Lazzati et al. 2017; Xiao et al. 2017; Zhang et al. 2017). We will investigate further this point in our future work.

Very possibly in the near future, more and more GWs' electromagnetic counterparts could be confirmed, produced by the compact binary mergers (especially for NS-NS and NS-BH). Noted that their optical/NIR emission might be originated from three mechanism: the ejecta or winds (kilonovae), the injection energy of magnetars (mergernovae), or the strong outflows from the hyperaccretion discs (quasi-SNe).

## ACKNOWLEDGEMENTS

We thank Zi-Gao Dai, Bing Zhang, and Tuan Yi for beneficial discussion and the anonymous referee for very useful suggestions and comments. This work was supported by the National Basic Research Program of China (973 Program) under grant 2014CB845800, the National Natural Science Foundation of China under grants 11473022 and U1431107, and the Fundamental Research Funds for the Central Universities (grant 20720160024).

## REFERENCES

- Abadie J., et al., 2010, *CQGra*, 27, 173001  
 Abbott B. P., et al., 2017, *PhRvL*, 119, 161101  
 Abbott B. P., et al., 2017, *ApJ*, 850, L40  
 Abbott B. P., et al., 2017, *ApJ*, 850, L39  
 Abramowicz M. A., Chen X., Kato S., Lasota J.-P., Regev O., 1995, *ApJ*, 438, L37  
 Alexander K. D., et al., 2017, *ApJ*, 848, L21  
 Aloy M. A., Janka H.-T., Müller E., 2005, *A&A*, 436, 273  
 Amati L., Guidorzi C., Frontera F., Della Valle M., Finelli F., Landi R., Montanari E., 2008, *MNRAS*, 391, 577  
 Amati L., Frontera F., Guidorzi C., 2009, *A&A*, 508, 173  
 Antonelli L. A., et al., 2009, *A&A*, 507, L45  
 Barkov M. V., Komissarov S. S., 2008, *MNRAS*, 385, L28  
 Barkov M. V., Komissarov S. S., 2010, *MNRAS*, 401, 1644  
 Bauswein A., Goriely S., Janka H.-T., 2013, *ApJ*, 773, 78  
 Begelman M. C., 2012, *MNRAS*, 420, 2912  
 Berger E., Fong W., Chornock R., 2013, *ApJ*, 774, L23  
 Berger E., et al., 2013, *ApJ*, 765, 121  
 Berger E., 2014, *ARA&A*, 52, 43  
 Blanchard P. K., et al., 2017, *ApJ*, 848, L22  
 Blandford R. D., Begelman M. C., 1999, *MNRAS*, 303, L1  
 Blandford R. D., Begelman M. C., 2004, *MNRAS*, 349, 68  
 Blandford R. D., McKee C. F., 1977, *MNRAS*, 180, 343  
 Blandford R. D., Payne D. G., 1982, *MNRAS*, 199, 883  
 Blandford R. D., Znajek R. L., 1977, *MNRAS*, 179, 433  
 Butler N. R., Kocevski D., Bloom J. S., Curtis J. L., 2007, *ApJ*, 671, 656  
 Burrows D. N., et al., 2005, *Sci*, 309, 1833  
 Campana S., et al., 2006, *Natur*, 442, 1008  
 Chawla S., Anderson M., Besselman M., Lehner L., Liebling S. L., Motl P. M., Neilsen D., 2010, *PhRvL*, 105, 111101  
 Cheung E., et al., 2016, *Natur*, 533, 504  
 Chincarini G., et al., 2010, *MNRAS*, 406, 2113  
 Chornock R., et al., 2017, *ApJ*, 848, L19  
 Connaughton V., 2002, *ApJ*, 567, 1028  
 Cowperthwaite P. S., et al., 2017, *ApJ*, 848, L17  
 Cummings J. R., et al., 2013, *GCN.1*, 15293, 1  
 Cutler C., Flanagan É. E., 1994, *PhRvD*, 49, 2658  
 Dai Z. G., Lu T., 1998, *A&A*, 333, L87  
 Dai Z. G., Wang X. Y., Wu X. F., Zhang B., 2006, *Sci*, 311, 1127  
 Della Valle M., et al., 2006, *Natur*, 444, 1050  
 Demianski M., Piedipalumbo E., Sawant D., Amati L., 2017, *A&A*, 598, A112  
 Di Matteo T., Perna R., Narayan R., 2002, *ApJ*, 579, 706  
 Dichiaro S., Guidorzi C., Amati L., Frontera F., Margutti R., 2016, *A&A*, 589, A97  
 Dietrich T., Bernuzzi S., Ujevic M., Brüggmann B., 2015, *PhRvD*, 91, 124041  
 Eggum G. E., Coroniti F. V., Katz J. I., 1988, *ApJ*, 330, 142  
 Eichler D., Livio M., Piran T., Schramm D. N., 1989, *Natur*, 340, 126  
 Evans P. A., et al., 2017, *arXiv*, arXiv:1710.05437  
 Fan Y.-Z., Wei D.-M., 2011, *ApJ*, 739, 47  
 Fan Y.-Z., Yu Y.-W., Xu D., Jin Z.-P., Wu X.-F., Wei D.-M., Zhang B., 2013, *ApJ*, 779, L25  
 Fong W., et al., 2017, *ApJ*, 848, L23  
 Foucart F., et al., 2014, *PhRvD*, 90, 024026  
 Fruchter A. S., et al., 2006, *Natur*, 441, 463  
 Fynbo J. P. U., et al., 2006, *Natur*, 444, 1047  
 Galama T. J., et al., 1998, *Natur*, 395, 670  
 Gal-Yam A., et al., 2006, *Natur*, 444, 1053  
 Gao H., Ding X., Wu X.-F., Dai Z.-G., Zhang B., 2015, *ApJ*, 807, 163  
 Gao H., Ding X., Wu X.-F., Zhang B., Dai Z.-G., 2013, *ApJ*, 771, 86  
 Gao H., Ren A.-B., Lei W.-H., Zhang B.-B., Lü H.-J., Li Y., 2017, *ApJ*, 845, 51  
 Gao H., Zhang B., Lü H.-J., Li Y., 2017, *ApJ*, 837, 50  
 Gehrels N., et al., 2006, *Natur*, 444, 1044  
 Ghirlanda G., Nava L., Ghisellini G., Celotti A., Burlon D., Covino S., Melandri A., 2012, *MNRAS*, 420, 483  
 Gorbovskoy E. S., et al., 2012, *MNRAS*, 421, 1874  
 Greiner J., et al., 2009, *ApJ*, 693, 1610  
 Gu W.-M., 2015, *ApJ*, 799, 71  
 Gu W.-M., Lu J.-F., 2007, *ApJ*, 660, 541  
 Guidorzi C., et al., 2009, *A&A*, 499, 439  
 Guidorzi C., et al., 2011, *MNRAS*, 417, 2124  
 Hallinan G., et al., 2017, *arXiv*, arXiv:1710.05435  
 Hawley J. F., Balbus S. A., Stone J. M., 2001, *ApJ*, 554, L49  
 Hjorth J., et al., 2003, *Natur*, 423, 847  
 Horesh A., Hotokezaka K., Piran T., Nakar E., Hancock P., 2016, *ApJ*, 819, L22  
 Horváth I., 2002, *A&A*, 392, 791  
 Hotokezaka K., Kiuchi K., Kyutoku K., Okawa H., Sekiguchi Y.-i., Shibata M., Taniguchi K., 2013, *PhRvD*, 87, 024001  
 Igumenshchev I. V., Narayan R., Abramowicz M. A., 2003, *ApJ*, 592, 1042  
 Janiuk A., Proga D., 2008, *ApJ*, 675, 519-527  
 Jiang Y.-F., Stone J. M., Davis S. W., 2014, *ApJ*, 796, 106  
 Jiang Y.-F., Stone J., Davis S. W., 2017, *arXiv*, arXiv:1709.02845  
 Jin Z.-P., Li X., Cano Z., Covino S., Fan Y.-Z., Wei D.-M., 2015, *ApJ*, 811, L22  
 Jin Z.-P., et al., 2016, *NatCo*, 7, 12898

- Just O., Bauswein A., Pulpillo R. A., Goriely S., Janka H.-T., 2015, *MNRAS*, 448, 541
- Kann D. A., et al., 2010, *ApJ*, 720, 1513
- Kann D. A., et al., 2011, *ApJ*, 734, 96
- Kasliwal M. M., Korobkin O., Lau R. M., Wollaeger R., Fryer C. L., 2017, *ApJ*, 843, L34
- Kawaguchi K., Kyutoku K., Nakano H., Okawa H., Shibata M., Taniguchi K., 2015, *PhRvD*, 92, 024014
- Kawaguchi K., Kyutoku K., Shibata M., Tanaka M., 2016, *ApJ*, 825, 52
- Kawanaka N., Piran T., Krolik J. H., 2013, *ApJ*, 766, 31
- Kilpatrick C. D., et al., 2017, *arXiv*, arXiv:1710.05434
- Kisaka S., Ioka K., Nakamura T., 2015, *ApJ*, 809, L8
- Kiuchi K., Sekiguchi Y., Kyutoku K., Shibata M., Taniguchi K., Wada T., 2015, *PhRvD*, 92, 064034
- Komissarov S. S., Barkov M. V., 2009, *MNRAS*, 397, 1153
- Kouveliotou C., Meegan C. A., Fishman G. J., Bhat N. P., Briggs M. S., Koshut T. M., Paciesas W. S., Pendleton G. N., 1993, *ApJ*, 413, L101
- Krühler T., et al., 2009, *A&A*, 508, 593
- Kulkarni S. R., 2005, *astro*, arXiv:astro-ph/0510256
- Kumar P., Zhang B., 2015, *PhR*, 561, 1
- Kyutoku K., Ioka K., Okawa H., Shibata M., Taniguchi K., 2015, *PhRvD*, 92, 044028
- Laskar T., Berger E., Margutti R., Perley D., Zauderer B. A., Sari R., Fong W., 2015, *ApJ*, 814, 1
- Lazzati D., Ramirez-Ruiz E., Ghisellini G., 2001, *A&A*, 379, L39
- Lazzati D., Deich A., Morsony B. J., Workman J. C., 2017, *MNRAS*, 471, 1652
- Lee H. K., Brown G. E., Wijers R. A. M. J., 2000, *ApJ*, 536, 416
- Lee H. K., Wijers R. A. M. J., Brown G. E., 2000, *PhR*, 325, 83
- Lei W. H., Wang D. X., Zhang L., Gan Z. M., Zou Y. C., Xie Y., 2009, *ApJ*, 700, 1970
- Lei W.-H., Zhang B., Liang E.-W., 2013, *ApJ*, 765, 125
- Lei W.-H., Zhang B., Wu X.-F., Liang E.-W., 2017, *ApJ*, 849, 47
- Levan A., Crowther P., de Grijs R., Langer N., Xu D., Yoon S.-C., 2016, *SSRv*, 202, 33
- Levesque E. M., et al., 2010, *MNRAS*, 401, 963
- Levesque E. M., Kewley L. J., 2007, *ApJ*, 667, L121
- Li L.-X., Paczyński B., 1998, *ApJ*, 507, L59
- Li L.-X., 2000, *PhRvD*, 61, 084016
- Li Y., Zhang B., Lü H.-J., 2016, *ApJS*, 227, 7
- Lipunov V. M., Postnov K. A., Prokhorov M. E., 1997, *MNRAS*, 288, 245
- Liu T., Gu W.-M., Xue L., Weng S.-S., Lu J.-F., 2008, *AIPC*, 1065, 298
- Liu T., Gu W.-M., Xue L., Lu J.-F., 2007, *ApJ*, 661, 1025
- Liu T., Gu W.-M., Xue L., Lu J.-F., 2012a, *Ap&SS*, 337, 711
- Liu T., Gu W.-M., Zhang B., 2017, *NewAR*, 79, 1
- Liu T., Hou S.-J., Xue L., Gu W.-M., 2015a, *ApJS*, 218, 12
- Liu T., Liang E.-W., Gu W.-M., Hou S.-J., Lei W.-H., Lin L., Dai Z.-G., Zhang S.-N., 2012b, *ApJ*, 760, 63
- Liu T., Lin Y.-Q., Hou S.-J., Gu W.-M., 2015b, *ApJ*, 806, 58
- Liu T., Lin C.-Y., Song C.-Y., Li A., 2017, *ApJ*, 850, 30
- Liu T., Song C.-Y., Zhang B., Gu W.-M., Heger A., 2018, *ApJ*, 852, 20
- Liu, T., Romero, G. E., Liu, M.-L., & Li, A. 2016, *ApJ*, 826, 82
- Lü H.-J., Zhang B., Liang E.-W., Zhang B.-B., Sakamoto T., 2014, *MNRAS*, 442, 1922
- Lü H.-J., Zhang H.-M., Zhong S.-Q., Hou S.-J., Sun H., Rice J., Liang E.-W., 2017, *ApJ*, 835, 181
- Ma S.-B., Lei W.-H., Gao H., Xie W., Chen W., Zhang B., Wang D.-X., 2018, *ApJ*, 852, L5
- MacFadyen A. I., Woosley S. E., 1999, *ApJ*, 524, 262
- Machida M., Matsumoto R., Mineshige S., 2001, *PASJ*, 53, L1
- Margutti R., et al., 2017, *ApJ*, 848, L20
- Margutti R., Guidorzi C., Chincarini G., Bernardini M. G., Genet F., Mao J., Pasotti F., 2010, *MNRAS*, 406, 2149
- Marshall F. E., et al., 2011, *ApJ*, 727, 132
- McKinney J. C., 2005, *ApJ*, 630, L5
- McKinney J. C., Tchekhovskoy A., Sadowski A., Narayan R., 2014, *MNRAS*, 441, 3177
- Metzger B. D., 2017, *LRR*, 20, 3
- Metzger B. D., Berger E., 2012, *ApJ*, 746, 48
- Metzger B. D., Fernández R., 2014, *MNRAS*, 441, 3444
- Metzger B. D., et al., 2010, *MNRAS*, 406, 2650
- Metzger B. D., Piro A. L., 2014, *MNRAS*, 439, 3916
- Moderski R., Sikora M., Lasota J. P., 1997, *rja.proc*, 110
- Mu H.-J., Gu W.-M., Hou S.-J., Liu T., Lin D.-B., Yi T., Liang E.-W., Lu J.-F., 2016a, *ApJ*, 832, 161
- Mu H.-J., et al., 2016b, *ApJ*, 831, 111
- Nagataki S., 2009, *ApJ*, 704, 937
- Nakamura T., Kashiyama K., Nakauchi D., Suwa Y., Sakamoto T., Kawai N., 2014, *ApJ*, 796, 13
- Nakar E., 2007, *PhR*, 442, 166
- Nakar E., Piran T., 2011, *Natur*, 478, 82
- Narayan R., Paczyński B., Piran T., 1992, *ApJ*, 395, L83
- Narayan R., Piran T., Kumar P., 2001, *ApJ*, 557, 949
- Narayan R., Yi I., 1995, *ApJ*, 444, 231
- Narayan R., Yi I., 1994, *ApJ*, 428, L13
- Nemmen R. S., Georganopoulos M., Guiriec S., Meyer E. T., Gehrels N., Sambruna R. M., 2012, *Sci*, 338, 1445
- Nicholl M., et al., 2017, *ApJ*, 848, L18
- Norris J. P., Gehrels N., Scargle J. D., 2011, *ApJ*, 735, 23
- Norris J. P., Gehrels N., Scargle J. D., 2010, *ApJ*, 717, 411
- Nousek J. A., et al., 2006, *ApJ*, 642, 389
- Oechslin R., Janka H.-T., 2006, *MNRAS*, 368, 1489
- Oechslin R., Janka H.-T., Marek A., 2007, *A&A*, 467, 395
- Ofek E. O., et al., 2007, *ApJ*, 662, 1129
- Ohsuga K., Mineshige S., 2011, *ApJ*, 736, 2
- Ohsuga K., Mori M., Nakamoto T., Mineshige S., 2005, *ApJ*, 628, 368
- Okuda T., 2002, *PASJ*, 54, 253
- Paczyński B., 1986, *ApJ*, 308, L43
- Paczyński B., 1991, *AcA*, 41, 257
- Pal'Shin V., et al., 2008, *GCN*, 8256, 1
- Pang B., Pen U.-L., Matzner C. D., Green S. R., Liebendörfer M., 2011, *MNRAS*, 415, 1228
- Parker M. L., et al., 2017a, *Natur*, 543, 83
- Parker M. L., et al., 2017b, *MNRAS*, 469, 1553
- Perley D. A., et al., 2009, *ApJ*, 696, 1871
- Pérez-Ramírez D., et al., 2010, *A&A*, 510, A105
- Piran T., Nakar E., Rosswog S., 2013, *MNRAS*, 430, 2121
- Popham R., Woosley S. E., Fryer C., 1999, *ApJ*, 518, 356
- Punsly, B., & Bini, D. 2016, *MNRAS*, 459, L41
- Racusin J. L., et al., 2009, *ApJ*, 698, 43
- Rhoads J. E., 1999, *ApJ*, 525, 737
- Rossi E. M., Begelman M. C., 2009, *MNRAS*, 392, 1451
- Rosswog S., 2007, *MNRAS*, 376, L48
- Rowlinson A., O'Brien P. T., Metzger B. D., Tanvir N. R., Levan A. J., 2013, *MNRAS*, 430, 1061
- Ryan G., van Eerten H., MacFadyen A., Zhang B.-B., 2015, *ApJ*, 799, 3
- Sądowski A., Narayan R., 2015, *MNRAS*, 453, 3213
- Sądowski A., Narayan R., McKinney J. C., Tchekhovskoy A., 2014, *MNRAS*, 439, 503
- Sakamoto T., et al., 2014, *GCN.1*, 16438, 1
- Savaglio S., Glazebrook K., Le Borgne D., 2009, *ApJ*, 691, 182
- Schutz B. F., 1989, *CQGra*, 6, 1761
- Shakura N. I., Sunyaev R. A., 1973, *A&A*, 24, 337
- Shappee B. J., et al., 2017, *arXiv*, arXiv:1710.05432
- Siegel D. M., Metzger B. D., 2017, *arXiv*, arXiv:1705.05473
- Smartt T. J., et al., 2017, *Natur*, 551, 75
- Song C.-Y., Liu T., Gu W.-M., Tian J.-X., 2016, *MNRAS*, 458, 1921
- Stanbro M., Meegan C., 2016, *GCN.1*, 19843, 1

- Stanek K. Z., et al., 2003, *ApJ*, 591, L17
- Stone J. M., Pringle J. E., Begelman M. C., 1999, *MNRAS*, 310, 1002
- Sun H., Zhang B., Gao H., 2017, *ApJ*, 835, 7
- Tanvir N. R., Levan A. J., Fruchter A. S., Hjorth J., Hounsell R. A., Wiersema K., Tunnicliffe R. L., 2013, *Natur*, 500, 547
- Tchekhovskoy A., McKinney J. C., 2012, *MNRAS*, 423, L55
- Thompson C., 1994, *MNRAS*, 270, 480
- Troja E., et al., 2007, *ApJ*, 665, 599
- Troja E., et al., 2017, *Natur*, 551, 71
- Tsutsui R., Yonetoku D., Nakamura T., Takahashi K., Morihara Y., 2013, *MNRAS*, 431, 1398
- Tutukov A. V., Yungelson L. R., Iben I., Jr., 1992, *ApJ*, 386, 197
- Usov V. V., 1992, *Natur*, 357, 472
- Wang Q. D., et al., 2013, *Sci*, 341, 981
- Woosley S. E., 1993, *ApJ*, 405, 273
- Woosley S. E., Bloom J. S., 2006, *ARA&A*, 44, 507
- Wu X. F., Dai Z. G., Wang X. Y., Huang Y. F., Feng L. L., Lu T., 2007, *AdSpR*, 40, 1208
- Xiao D., Liu L.-D., Dai Z.-G., Wu X.-F., 2017, *ApJ*, 850, L41
- Xin L.-P., et al., 2011, *MNRAS*, 410, 27
- Xu D., et al., 2009, *ApJ*, 696, 971
- Yang B., et al., 2015, *NatCo*, 6, 7323
- Yasuda T., Urata Y., Enomoto J., Tashiro M. S., 2017, *MNRAS*, 466, 4558
- Yi S.-X., Xi S.-Q., Yu H., Wang F. Y., Mu H.-J., Lü L.-Z., Liang E.-W., 2016, *ApJS*, 224, 20
- Yi T., Gu W.-M., Yuan F., Liu T., Mu H.-J., 2017, *ApJ*, 836, 245
- Yi T., Gu W.-M., Liu T., Kumar R., Mu H.-J., Song C.-Y., 2018, *MNRAS*,
- Yu Y.-W., Zhang B., Gao H., 2013, *ApJ*, 776, L40
- Yuan F., Bu D., Wu M., 2012, *ApJ*, 761, 130
- Yuan F., Narayan R., 2014, *ARA&A*, 52, 529
- Yuan F., Wu M., Bu D., 2012, *ApJ*, 761, 129
- Zaninoni E., Bernardini M. G., Margutti R., Amati L., 2016, *MNRAS*, 455, 1375
- Zhang B.-B., et al., 2017, *arXiv*, arXiv:1710.05851
- Zhang B.-B., Zhang B., Murase K., Connaughton V., Briggs M. S., 2014, *ApJ*, 787, 66
- Zhang, B.-B. 2011, Ph.D. Thesis
- Zhang B., 2013, *ApJ*, 763, L22
- Zhang B., et al., 2007, *ApJ*, 655, 989
- Zhang B., Mészáros P., 2001, *ApJ*, 552, L35
- Zhang B., Zhang B.-B., Liang E.-W., Gehrels N., Burrows D. N., Mészáros P., 2007, *ApJ*, 655, L25
- Zhang B., et al., 2009, *ApJ*, 703, 1696
- Zhang F.-W., Shao L., Yan J.-Z., Wei D.-M., 2012, *ApJ*, 750, 88

This paper has been typeset from a  $\text{\TeX}/\text{\LaTeX}$  file prepared by the author.